Chapter

Modeling Lost-Circulation into Fractured Formation in Rock Drilling Operations

Rami Albattat and Hussein Hoteit

Abstract

Loss of circulation while drilling is a challenging problem that may interrupt drilling operations, reduce efficiency, and increases cost. When a drilled borehole intercepts conductive faults or fractures, lost circulation manifests as a partial or total escape of drilling, workover, or cementing fluids into the surrounding rock formations. Studying drilling fluid loss into a fractured system has been investigated using laboratory experiments, analytical modeling, and numerical simulations. Analytical modeling of fluid flow is a tool that can be quickly deployed to assess lost circulation and perform diagnostics, including leakage rate decline and fracture conductivity. In this chapter, various analytical methods developed to model the flow of non-Newtonian drilling fluid in a fractured medium are discussed. The solution methods are applicable for yield-power-law, including shear-thinning, shear-thickening, and Bingham plastic fluids. Numerical solutions of the Cauchy equation are used to verify the analytical solutions. Type-curves are also described using dimensionless groups. The solution methods are used to estimate the range of fracture conductivity and time-dependent fluid loss rate, and the ultimate total volume of lost fluid. The applicability of the proposed models is demonstrated for several field cases encountering lost circulations.

Keywords: lost-circulation, mud loss, leakage, fractures, Herschel-Bulkley, yield-power law, Cauchy momentum equation, type-curves, non-Newtonian fluids

1. Introduction

Drilling technology has been widely deployed in many industries, such as oil and gas, geothermal, environmental remediation, mining, carbon dioxide sequestration, gas storage, water well, infrastructure development, among others [1]. In many situations, drilling entails various technical challenges and difficulties, often causing economic, safety, and environmental disturbances. Due to the complex nature of subsurface geological formations, technical problems often emerge unexpectedly. One of the most pressing problems is lost circulation into fractured formation. Preserving the drilling fluid within the borehole is crucial for removing cuttings, lubrication, hydraulic rotations, pressure control, among others. Fluid total or partial loss into the wellbore surrounding formation may result in wellbore instability.

Drilling fluid-loss is a costly problem. This phenomenon may obstruct operations, increase the nonproductive time (NPT), contaminate water tables, and cause formation damage and safety hazard [2–9]. Drilling fluid typically accounts for

25–40% of the total drilling costs [8]. Furthermore, lost circulation may cause other issues, such as wellbore instability, sloughing shale, and washout [10]. Such problems cost the industry about one billion US dollars per annum worldwide [11, 12]. For instance, a study including 1500 gas wells in the Gulf of Mexico showed that lost-circulation accounts for 13% of the total drilling problems [5], as appears in **Figure 1**. Another study for 103 wells in the Duvernay area in Canada reported a loss of $2.6 million and 27.5 days of NPT because of lost circulation (**Figure 2**). In the Middle East, a group of 144 wells in Rumaila field, Iraq, encountered major lost-circulation problems [14], causing 48% of all drilling issues and loss of 295 days NPT, as illustrated in **Figure 3**. This high occurrence of lost-circulation was attributed to the presence of conductive natural fractures in the carbonate formations. For instance, more than 35% of drilled wells in a fractured carbonate formation in Iran experienced lost circulation [15]. Similarly, in Saudi Arabia, one-third of the

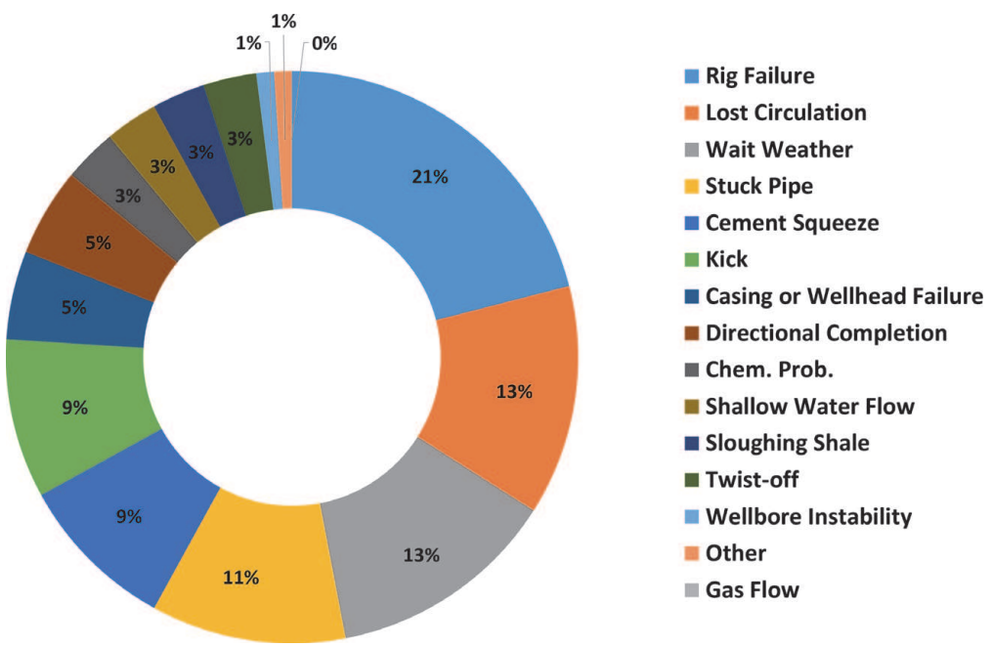

Figure 1.
Contribution of various drilling problems reported for 1500 wells in the Gulf of Mexico [5], where lost circulation accounts for 13% of the total.

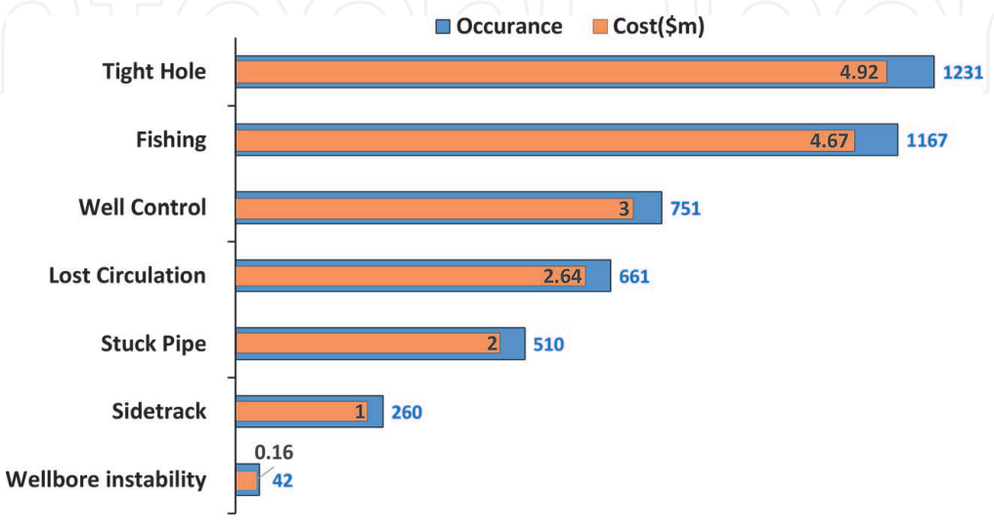

Figure 2.
Cost overhead from various drilling problems for 103 wells in the Duvernay area in Canada [13], where lost circulation account for $2.6 m.

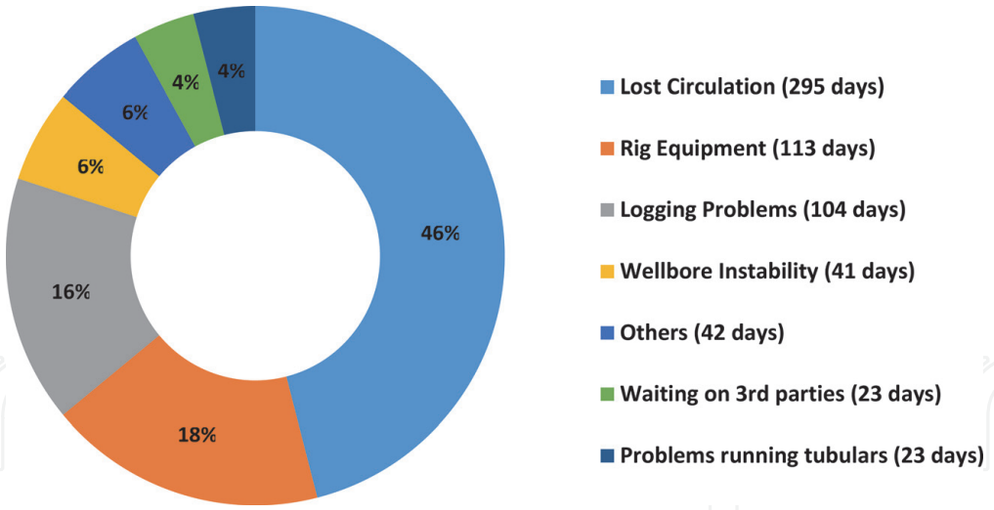

Figure 3.
Contribution of various drilling problems to NPT in the Rumaila field in Iraq, total lost circulation is the top drilling issue encountered in that field, data source from [14].

drilled well underwent lost circulation [16]. Lost circulation has also been reported in other places [17, 18].

Lost circulation can be classified based on the severity of the flow loss rate [19], as shown in **Table 1**. These categories provide general guidance to set the mitigation plan depending on the severity of the fluid loss. Seepage loss can sometimes be tolerable to continue drilling without interruption. However, major loss demands a careful response to regain a full circulation fluid.

Fluid loss is often encountered in fractured formations, which can be subdivided into four types: induced-drilling fracture, caves or vugs, natural fracture, and high permeable formation [20]. An illustration of the four types is shown in **Figure 4**. Each formation type exhibits different fluid loss behavior and, therefore, may require a specific mitigation plan.

Naturally fractured formation, which is the focus of this chapter, is often prone to severe loss during either drilling, cementing, or completion/workover job [21]. Consequently, multiple problems may emanate because of the loss severity, such as kicks, wellbore instability, environmental contamination, and formation damage. To mitigate this problem, one procedure is to add lost circulation material (LCM) to the circulation fluid [22–25]. The LCM fluid properties such as viscosity and density are selected according to the formation type and the subsurface conditions, such as the depth, pressure, and fracture conductivity, among other factors [26]. Fluid loss rate into natural fractures mostly commences with a sudden spurt followed by a gradual declining loss [27]. The ultimately lost volume is dependent on several factors, such as fluid mobility, fracture conductivity, pore-volume, and fracture extension [28].

Because of the nature of this problem that requires immediate intervention, there is a need in the industry to establish an accurate and efficient modeling tool

Lost Type	Flow Rate Amount
Seepage loss	Less than 1.5 m^3/hr
Partial loss	1.5 to 15 m^3/hr
Severe loss	15 to 75 m^3/hr
Total loss	No return to surface

Table 1.
Classification of lost-circulation severity [19].

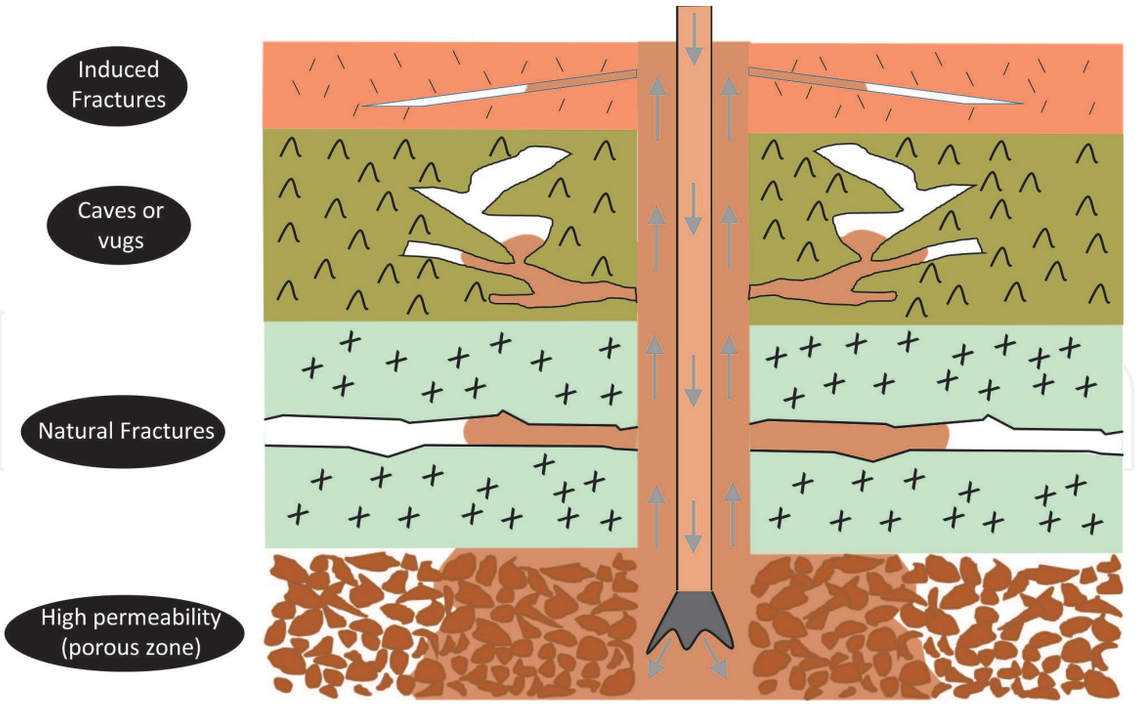

Figure 4.
Four types of rock formations causing loss-circulation. The arrows indicate the direction of circulating fluid starting from the surface within the drill pipe going to the open-hole and to the annulus of the wellbore back to the surface.

that is feasible at real-time drilling operations to perform diagnostics and predictions.

During the last two decades, many analytical solutions have been introduced in the literature to model mud loss into fractured formation. Early modeling attempts for simplified fractured cases were based on Darcy's Law at steady-state conditions [29, 30]. Afterward, a semi-analytical solution was introduced for the Newtonian fluid model into a horizontal fracture by combining the diffusivity equation and mass conservation in a one-dimensional (1D) radial system [31]. Since this derived ordinary differential equation (ODE) was solved numerically, an analytical solution of the diffusivity equation for a fluid with a constant viscosity at steady-state conditions was introduced [32]. Another approach based on type-curves, which were generated by numerical solutions to describe mud loss volume as a function of time into a horizontal fracture, was established [33]. The type-curves are applicable for non-Newtonian fluid and follow a model that exhibits Bingham plastic rheological behavior. The numerically generated type-curves are based on dimensionless parameters that depend on the effective fracture hydraulic aperture, fluid properties, and differential pressure. However, these models inherit the limitations of numerical methods in introducing numerical artifacts such as numerical dispersion and grid dependency. Later, an analytical solution was proposed [34, 35]. Estimation of hydraulic fracture aperture by simplifying insignificant terms in the final equation form was analyzed [36]. Following the same workflow, a solution was developed based on Yield-Power-Law fluid by reducing a Taylor expansion of the governing nonlinear flow equation into its linear terms [37].

This chapter is intended to give an overview of laboratory and modeling tools applicable for lost circulation in fractured media. Two main subjects are discussed. First, the governing equations to model non-Newtonian fluid in a fractured system are reviewed. We then introduce the solution method to develop a semi-analytical solution to model drilling fluid loss. The fluid exhibits a Herschel-Bulkley behavior, where the Cauchy equation of motion is used to describe the fluid flow. Due to the

nonlinearity of the problem, the system of equations is reformulated and transformed into ODE's, which is then computed numerically with an efficient ODE solver [38]. Based on the semi-analytical solution, type-curves are generated, capturing dimensionless fluid loss volume as a function of time. High-resolution finite element methods are used to verify the analytical approach. The applicability of the method is then demonstrated for field cases exhibiting loss of circulation, where formation and fluid uncertainties are addressed with Monte Carlo simulations. In the second subject, an experimental study designed to mimic fluid leakage in a horizontal fracture is discussed. These experiments are used to study the steady-state flow conditions of non-Newtonian fluids into the fracture and demonstrate the flow stoppage process. Simulations are used to replicate the physics, including the effect of fracture deformation. Type-curves are also derived from Cauchy equation of motion to capture the effect of fracture ballooning.

2. Mud invasion into a fractured system

Various studies have been conducted in the literature to investigate the flow behavior of drilling fluids in fractured systems [39–41], where a horizontal, radial fracture is considered, as shown in **Figure 5**. The choice of the fracture geometry is motivated by its convenience to be replicated with experimental apparatus and analytical modeling. Even though the fracture geometry may seem simplistic, it can provide useful insights at lab and field scales [43, 44].

Consider two parallel radial plates to mimic a horizontal fracture, intercepting a wellbore, as illustrated in **Figure 5**. Note that horizontal fractures could occur at shallow depths and over-pressurized formations [45, 46].

The general governing equation describing the dynamics of non-Newtonian fluid flow in an open fracture is given by the Cauchy momentum Equation [47, 48], such that,

$$\rho \frac{\partial \mathbf{v}}{\partial t} + \rho(\mathbf{v} \cdot \nabla)\mathbf{v} = \nabla \cdot (-p\mathbf{I} + \boldsymbol{\tau}) + \rho \mathbf{g}, \tag{1}$$

Where p denotes the fluid pressure, t is time, $\boldsymbol{\tau}$ is the shear stress, $\mathbf{g}$ is the gravity term, ρ is the density, $\mathbf{I}$ is identity matrix, and $\mathbf{v}$ is the flow velocity. Divergence delta operator is $\nabla\cdot$.

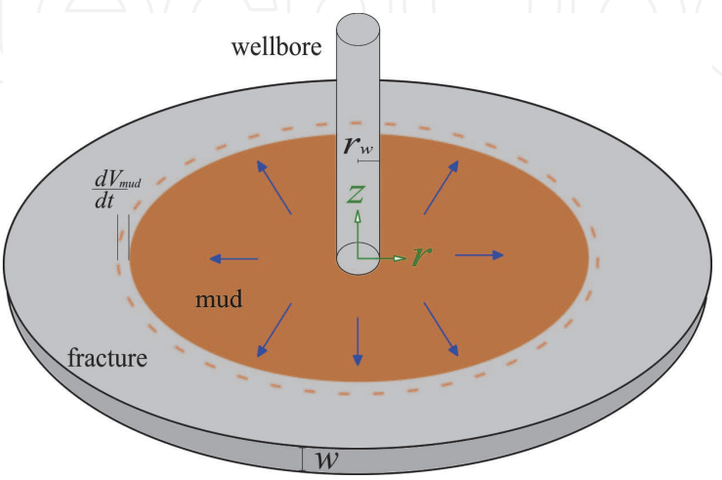

Figure 5.
Physical domain illustrating a horizontal fracture intercepted by a wellbore. The shaded brown area reflects the invaded mud zone, r_w is the wellbore radius, w is the fracture aperture, V_{mud} is the mud loss volume, and t is the time [42].

Assuming steady-state conditions and neglecting the gravity and inertial effects, Eq. (1) simplifies to,

$$0 = \nabla \cdot (-p\mathbf{I} + \boldsymbol{\tau}), \tag{2}$$

The above equation reduces into two fundamental forces; pressure forces and shear stress force. In a 1D radial system with polar coordinates, Eq. (2) simplifies to (see [49]),

$$\tau(z, r) = z\frac{\partial p}{\partial r}, \tag{3}$$

Where $\tau(z, r)$ is the radial shear stress component perpendicular to the z-directionand r is radial distance which is the variable argument.

On the other hand, the Herschel-Bulkley model is expressed by [50],

$$\tau(z, r) = \tau_0 + m\left(\frac{dv_r}{dz}\right)^n. \tag{4}$$

The fluid yield stress, which determines the fluidity state, is denoted by τ_0, and the consistency multiplier and behavioral flow index are $m$and n, respectively. The flow index is a positive number, reflecting the fluid rheological behavior where shear-thinning ($n < 1$) and shear-thickening ($n > 1$) can occur. Typical values of this dimensionless parameter for drilling fluids range from 0.3 to 1.0 [51]. Shear rate, which is the derivative of the radial velocity v_r in the z-direction, is nonlinear due to the flow index.

The mechanisms corresponding to the solution method of the mud invasion phenomenon in a fractured system are shown on a cross-section in **Figure 6**. The radial velocity decreases as the fluid propagates away from the wellbore within the fracture, and therefore shear stress lessens. Therefore, shear-thinning is expected to be maximum near the wellbore and reduces gradually with radial distance, which induces shear-thickening from yield stress. Furthermore, flow velocity and shear stress variations in the z-direction create layers of fluid rheological properties and fluid self-friction that becomes maximum at the walls of the fracture. Fluid self-friction is minimum at the centerline of the fracture, as shown in **Figure 6**, resulting in a region at the fracture center with zero shear rate, that is, $dv_r/dz = 0$. In this zone, the yield shear stress corresponds to τ_0(see Eq. (4)). This fluid flow region in the fracture is subdivided into plug-flow and free-flow regions. The plug-region extends toward the walls of the fracture as the shear-stress reduces, and the fluid flows further from the wellbore. The plug region can eventually reach the fracture wall leading to a complete stoppage of the fluid leakage (see **Figure 7a**). In other words,

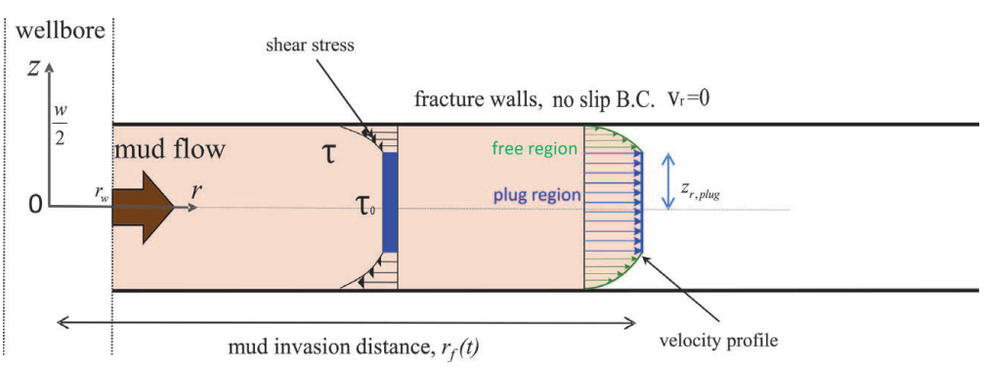

Figure 6.
Illustration of an infinite-acting fracture of aperture w, intercepting a wellbore with radius r_w. No-flow and no-slip boundary conditions are imposed at the fracture wall. Mud-front distance $r_f(t)$ is a time-dependent parameter.

mud leakage stalls in the fracture when the pressure gradient between the fracture inlet and the mud front becomes smaller than the yield stress τ_0 (see **Figure 7b**).

The following boundary conditions are considered for the two flow regions,

$$v_r(z) = \begin{cases} v_{r,plug}(z), & for \quad z \le z_{plug} \\ v_{r,free}(z), & for \quad z_{plug} < z < \dfrac{w}{2} \\ 0, & for \quad z = \dfrac{w}{2} \end{cases} \tag{5}$$

In the above equation, z_{plug} represents the extension of the plug region in the z-direction. $v_{r,plug}$, and $v_{r,free}$ are, respectively, the flow velocities within the plug- and free-region. The no-slip boundary condition is described by the last equation in (5).

Eq. (4) and Eq. (3) are combined to express the solution of the velocity, such that,

$$v_r(z) = \frac{n\left(-\frac{\partial p}{\partial r}\frac{w}{2} + \tau_0\right)\left(\frac{\frac{\partial p_w}{\partial r}2 - \tau_0}{m}\right)^{1/n} + n\left(-\frac{\partial p}{\partial r}z + \tau_0\right)\left(\frac{\frac{\partial p}{\partial r}z - \tau_0}{m}\right)^{\frac{1}{n}}}{\frac{\partial p}{\partial r}(n+1)} \tag{6}$$

The plug-region is modeled by imposing the condition, $dv_r/dz = 0$. Therefore, Eq. (6) can be expressed for each region individually, as follows,

$$\begin{aligned} v_{r,free}(z) &= \frac{n}{n+1}\left(z_{plug} - \frac{w}{2}\right)\left(\frac{\frac{\partial p}{\partial r}\left(\frac{w}{2} - z_{plug}\right)}{m}\right)^{1/n} + \frac{n}{n+1}\left(z - z_{plug}\right)\left(\frac{\frac{\partial p}{\partial r}\left(z - z_{plug}\right)}{m}\right)^{\frac{1}{n}} \\ v_{r,plug}(z) &= \frac{n}{n+1}\left(\frac{\tau_0}{\frac{\partial p}{\partial r}} - \frac{w}{2}\right)\left(\frac{\left(\frac{w}{2}\frac{\partial p}{\partial r} - \tau_0\right)}{m}\right)^{1/n} \end{aligned} \tag{7}$$

From the definition of the total volumetric flow rate Q_{total}, one obtains,

$$Q_{total} = Q_{plug} + Q_{free} \tag{8}$$

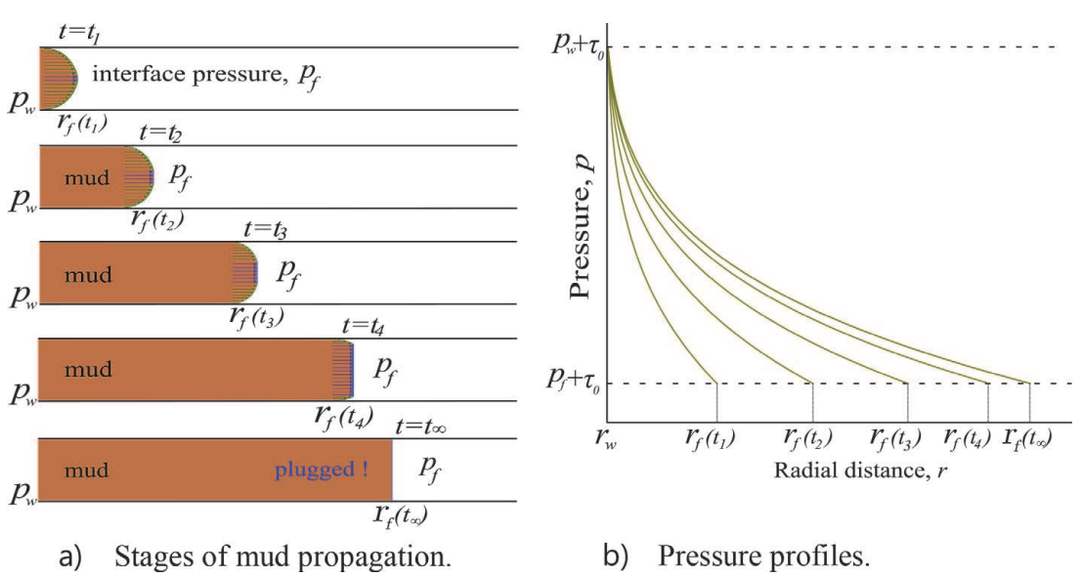

Figure 7.
Illustration of yield-power-law fluid flow in a radial fracture showing the evolution of the propagation of the plug region as the mud travels away from the wellbore, resulting in total plugging (a). Plot (b) shows typical pressure profiles versus radial distance at various times and invasion distances.

Applying surface integral,

$$Q_{total} = 4\pi r \int_{0}^{z_{plug}} v_{r,plug} dz + 4\pi r \int_{z_{plug}}^{w/2} v_{r,free} dz \tag{9}$$

Substituting Eq. (7) into Eq. (9) and arranging to obtain,

$$Q_{total}^{n} = \frac{(4\pi r)^{n}}{m}\left(\frac{w}{2}\right)^{2n+1}\left(\frac{n}{2n+1}\right)^{n}\left(\frac{dp}{dr}\right)\left(1-\frac{\tau_0}{\frac{w}{2}\frac{dp}{dr}}\right)\left(1-\left(\frac{1}{n+1}\right)\frac{\tau_0}{\frac{w}{2}\frac{dp}{dr}}-\left(\frac{n}{n+1}\right)\left(\frac{\tau_0}{\frac{w}{2}\frac{dp}{dr}}\right)^{2}\right)^{n} \tag{10}$$

The above equation is rearranged with the following quadratic equation to express the pressure term explicitly, that is,

$$\left(\frac{dp}{dr}\right)^{2} - \left(\frac{Q_{total}^{n}}{r^{n}A} + B\right)\frac{dp}{dr} + D = 0 \tag{11}$$

Where,

$$A = \frac{(4\pi)^{n}}{m}\left(\frac{w}{2}\right)^{2n+1}\left(\frac{n}{2n+1}\right)^{n}; B = \left(\frac{2n+1}{n+1}\right)\frac{\tau_0}{w/2}; D = \left(\frac{n-n^{2}}{n+1}\right)\left(\frac{\tau_0}{w/2}\right)^{2}$$

Solving the differential pressure and integrating along the radial domain by implementing a moving boundary condition, a final ODE system is reached, as follows,

$$\begin{cases} p_f - p_w = \dfrac{B\left(r_f(t) - r_w\right)}{2} + \dfrac{Q_{total}^{n}\left(r_f(t)^{1-n} - r_w^{1-n}\right)}{2(1-n)A} + \dfrac{1}{2}\displaystyle\int_{r_w}^{r_f(t)}\left(\sqrt{\left(B + \frac{Q_{total}^{n}}{r^{n}A}\right)^{2} - 4D}\right)dr \\ Q_{total} = 2\pi w r_f(t)\dfrac{dr_f(t)}{dt} \end{cases} \tag{12}$$

Eq. (12) is nonlinear for a general value of n, and it cannot be solved analytically. However, a general semi-analytical solution can be derived [42]. This solution is a generalization to other particular solutions in the literature. For instance, when $n = 1$, reflecting a Bingham plastic fluid, a closed-form solution can be obtained, as demonstrated by Lietard *et al.* [33]. **Figure 8** shows that the proposed general semi-analytical solution is in perfect agreement with the analytical solution by Lietard *et al.* [33]. For general cases of n, numerical simulations could be used to verify the semi-analytical model, as shown in **Figure 9**.

2.1 Dimensionless type-curves

For general applications, type-curves are used as a diagnostic tool to assess the solution by matching the trends of observed data to the type-curves. This approach is commonly used in well testing [52]. To enable scalability of the solution for a wide range of problem conditions, type-curves are expressed in terms of dimensionless groups. In this problem, the following dimensionless variables are considered,

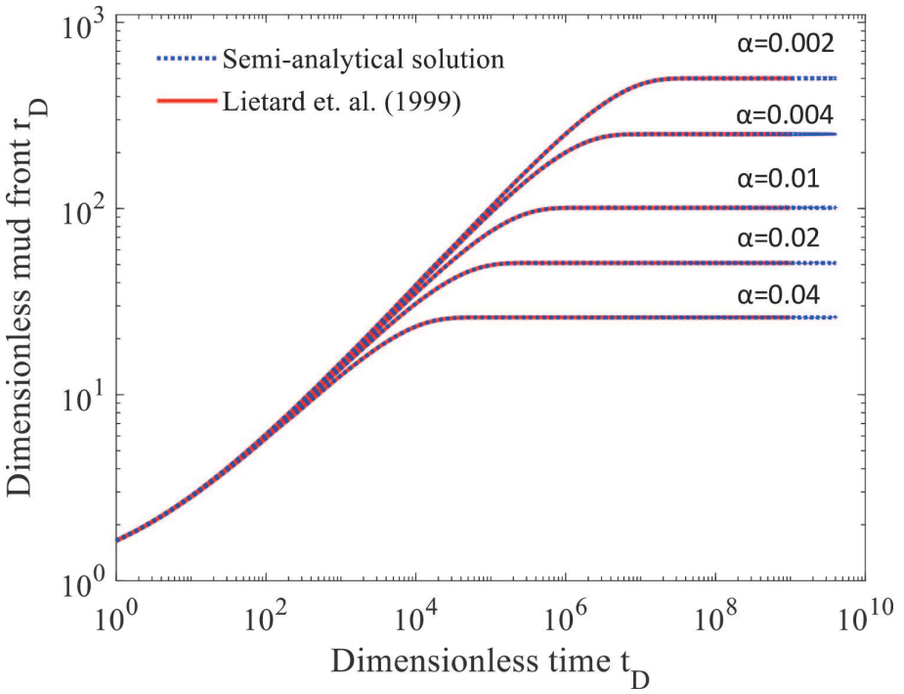

Figure 8.
Proposed semi-analytical solution compared with Liétard et al. (1999) for a Bingham plastic fluid [42].

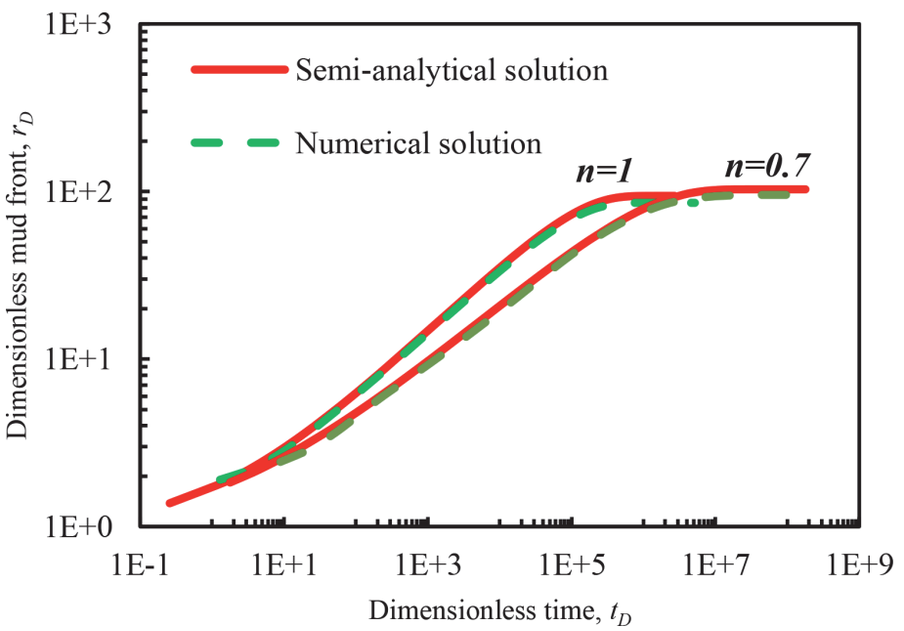

Figure 9.
Proposed semi-analytical solution compared with a finite-element model showing a good agreement [42].

$$
\begin{aligned}
r_D &= \frac{r_f}{r_w} \\
V_D &= \frac{V_m}{V_w} = \frac{\pi w\left(r_f{}^2 - r_w{}^2\right)}{\pi w r_w{}^2} = \left(\frac{r_f}{r_w}\right)^2 - 1 = r_D{}^2 - 1 \\
\alpha &= \left(\frac{2n+1}{n+1}\right)\left(\frac{2r_w}{w}\right)\left(\frac{\tau_0}{\Delta p}\right) \\
\beta &= \left(\frac{n}{2n+1}\right)\left(\frac{w}{r_w}\right)^{1+\frac{1}{n}}\left(\frac{\Delta p}{m}\right)^{\frac{1}{n}} \\
t_D &= t\beta
\end{aligned}
\tag{13}
$$

[18] Schlumberger, Lost Circulation Solution Saves Time and USD 3.3 Million for Chevron, Schlumberger. (2011).

[19] E.B. Nelson, D. Guillot, Well Cementing: Second Edition, Schlumberger, Texas, 2006.

[20] A. Lavrov, Lost circulation: Mechanisms and solutions, 2016. h ttps://doi.org/10.1016/C2015-0-00926-1.

[21] V. Dokhani, Y. Ma, Z. Li, T. Geng, M. Yu, Transient effects of leak-off and fracture ballooning on mud loss in naturally fractured formations, 53rd U. S. Rock Mech. Symp. (2019).

[22] A. Ali, C.L. Kalloo, U.B. Singh, Preventing lost circulation in severely depleted unoonsolidated sandstone reservoirs, SPE Repr. Ser. (1997) 103–109. doi:10.1016/0148-9062(94)91150-9.

[23] D.J. Attong, U.B. Singh, G. Teixeira, Successful use of a modified MWD tool in a high-concentration LCM mud system, SPE Drill. Complet. 10 (1995) 22–26. doi:10.2118/25690-PA.

[24] K. Knudsen, G.A. Leon, A.E. Sanabria, A. Ansari, R.M. Pino, First application of thermal activated resin as unconventional LCM in the Middle East, Soc. Pet. Eng. - Abu Dhabi Int. Pet. Exhib. Conf. ADIPEC 2015. (2015) 1–8. doi:10.2118/177430-ms.

[25] M. Olsen, G. Lende, K. Rehman, P. Haugum, J. Mo, G. Smaaskjar, R. Næss, Innovative and established LCM cementing solutions combined to create novel LCM cementing fluid train, Soc. Pet. Eng. - SPE Norw. One Day Semin. 2019. (2019). doi:10.2118/195622-ms.

[26] J. Luzardo, E.P. Oliveira, P.W.J. Derks, R.V. Nascimento, A.P. Gramatges, R. Valle, I.G. Pantano, F. Sbaglia, K. Inderberg, Alternative lost circulation material for depleted reservoirs, in: OTC Bras., Offshore Technology Conference, 2015. doi: 10.4043/26188-MS.

[27] C.G. Dyke, Bailin Wu, D. Milton-Taylor, Advances in characterizing natural-fracture permeability from mud- log data, SPE Form. Eval. 10 (1995) 160–166. doi:10.2118/25022-pa.

[28] J. NORMAN, Coriolis sensors open lines to real-time data, Drill. Contract. 67 (2011) 0–3.

[29] C.E. Bannister, V.M. Lawson, Role of cement fluid loss in wellbore completion, Proc. - SPE Annu. Tech. Conf. Exhib. 1985-Septe (1985). doi: 10.2523/14433-ms.

[30] R. Bruckdorfer, A. Gleit, Static Fluid Loss Model, SPE Gen. (1988) 20. https:// doi.org/.

[31] F. Sanfillippo, M. Brignoli, F.J. Santarelli, C. Bezzola, Characterization of Conductive Fractures While Drilling, SPE Eur. Form. Damage Conf. (1997) 319–328. doi:10.2118/38177-ms.

[32] R. Maglione, A. Marsala, Drilling mud losses: problem analysis, AGIP Internal Report, 1997.

[33] O. Liétard, T. Unwin, D.J. Guillot, M.H. Hodder, Fracture width logging while drilling and drilling mud/loss-circulation-material selection guidelines in naturally fractured reservoirs, SPE Drill. Complet. 17 (1999) 237–246.

[34] F. Civan, M. Rasmussen, Further discussion of fracture width logging while drilling and drilling mud/loss-circulation-material selection guidelines in naturally fractured reservoirs, SPE Drill. Complet. 17 (2002) 249–250.

[35] S. Sawaryn, Discussion of fracture width logging while drilling and drilling mud/loss-circulation-material selection guidelines in naturally fractured

reservoirs, SPE Drill. Complet. 4 (2002) 247–248.

[36] J. Huang, D.V. Griffiths, S.-W. Wong, Characterizing Natural-Fracture Permeability From Mud-Loss Data, SPE J. 16 (2011) 111–114. doi:10.2118/139592-PA.

[37] Majidi, S.Z. Miska, M. Yu, L.G. Thompson, J. Zhang, Quantitative Analysis of Mud Losses in Naturally Fractured Reservoirs: The Effect of Rheology, SPE Drill. Complet. December 2 (2010) 509–517. doi: 10.2118/114130-PA.

[38] A.C. Hindmarsh, P.N. Brown, K.E. Grant, S.L. Lee, R. Serban, D.E. Shumaker, C.S. Woodward, SUNDIALS: Suite of nonlinear and differential/ algebraic equation solvers, ACM Trans. Math. Softw. 31 (2005) 363–396. doi: 10.1145/1089014.1089020.

[39] A. Nasiri, A. Ghaffarkhah, M. Keshavarz Moraveji, A. Gharbanian, M. Valizadeh, Experimental and field test analysis of different loss control materials for combating lost circulation in bentonite mud, J. Nat. Gas Sci. Eng. 44 (2017) 1–8. doi:10.1016/j. jngse.2017.04.004.

[40] S. Yousefirad, E. Azad, M. Dehvedar, P. Moarefvand, The effect of lost circulation materials on differential sticking probability: Experimental study of prehydrated bentonite muds and Lignosulfonate muds, J. Pet. Sci. Eng. 178 (2019) 736–750.

[41] M. Khafaqa, Experimental Study on Effectiveness of Lost Circulation Materials to Mitigate Fluid Losses, MONTANUNIVERSITÄT LEOBEN, 2016.

[42] R. Albattat, H. Hoteit, A Semi-Analytical Approach to Model Drilling Fluid Leakage Into Fractured Formation, 2020. https: //doi.org/ https://arxiv.org/abs/2011.04746.

[43] H. Hoteit, A. Firoozabadi, An efficient numerical model for incompressible two-phase flow in fractured media, Adv. Water Resour. 31 (2008) 891–905. doi:10.1016/j. advwatres.2008.02.004.

[44] B. Koohbor, M. Fahs, H. Hoteit, J. Doummar, A. Younes, B. Belfort, An advanced discrete fracture model for variably saturated flow in fractured porous media, Adv. Water Resour. 140 (2020) 103602. doi:10.1016/j. advwatres.2020.103602.

[45] M.B. Smith, C.T. Montgomery, Hydraulic fracturing, Crc Press, 2015. doi:10.1201/b16287.

[46] Z. Ben-Avraham, M. Lazar, Z. Garfunkel, M. Reshef, A. Ginzburg, Y. Rotstein, U. Frieslander, Y. Bartov, H. Shulman, Structural styles along the Dead Sea Fault, in: D.G. Roberts, A.W.B. T.-R.G. and T.P.P.M. Bally Cratonic Basins and Global Tectonic Maps (Eds.), Reg. Geol. Tectonics, Elsevier, Boston, 2012: pp. 616–633. doi:10.1016/B978-0-444-56357-6.00016-0.

[47] F. Irgens, Rheology and non-newtonian fluids, Springer International Publishing, 2014.

[48] D. Cioranescu, V. Girault, K.R. Rajagopal, Mechanics and Mathematics of Fluids of the Differential Type, Springer, 2016. doi:10.1007/978-3-319-39330-8.

[49] R.L. Panton, Incompressible flow, John Wiley & Sons, 2013. https://doi.org/https://doi.org/10.1002/9781118713075.ch10.

[50] T. Hemphil, A. Pilehvari, W. Campos, Yield-power law model more accurately predicts mud rheology, Oil Gas J. 91 (1993) 45–50.

[51] V.C. Kelessidis, R. Maglione, C. Tsamantaki, Y. Aspirtakis, Optimal determination of rheological parameters